

## Numerical and Experimental Studies of Two-Phase Flow in Cooled / and Adiabatic Capillary Tubes

Dr. Wahid S. Mohammad \*, Dr. Nazar F. Antwan\*  
& Zainalabdeen Hussein Obeed\*

Received on: 18/10/2009

Accepted on: 6/5/2010

### Abstract

A numerical and experimental study was performed to predict the flow and thermal performance of a capillary tube that used in air conditioning and refrigeration systems. In the numerical study, the (CFD) technique was employed to model the problem using the finite volume method for a two-phase, two dimensional flow in the pipe. In the experimental part, an experimental rig was constructed using a split unite to measure the temperature and pressure along the capillary tube. These measurements were taken for (R-22) refrigerant with different ambient temperatures. It was found that for a fixed length and diameter of capillary tube the mass flow rate of (R-22) increases as the inlet temperature increases. The numerical study was then applied to predict the flow and heat transfer along several types of capillary tube, i.e. several lengths, diameters, and refrigerants, for cooled and non cooled tube. In the non cooled capillary results, the capillary tube length of R-407C (R-32/125/134a(23/25/52)) was found to be shorter than that required for (R-22). It was also found that (R-22) vaporized later than its corresponding (R-407C). The same condition was found for (R-12) and its alternative R-134a (CF3CH2F). The numerical results show a large effect of the length of capillary tube on the refrigeration system performance. When the length increases, the drop in pressure, temperature, and density decreases, while the velocity and dryness fraction increases.

### دراسة نظرية وعملية للجريان ثنائي الطور لموائع التثليج في الانابيب الشعرية المعزولة/والمبردة

#### الخلاصة

تم اجراء دراسة نظرية وعملية للتعرف على اداء الانبوب الشعري المستخدم في منظومات التثليج وتكييف الهواء وتضمنت الدراسة النظرية حل المشكلة باستخدام تقنية (CFD) بالاعتماد على طريقة الحجم المحددة للجريان ثنائي الطور ثنائي الابعاد داخل الانبوب الشعري. في الجزء العملي تم تحويل واستخدام وحدة تبريد لقياس درجة الحرارة والضغط على طول الانبوب الشعري. اخذت هذه القياسات لمائع التثليج (R-22) عند درجات حرارة مختلفة للمحيط. توصلت الدراسة الى ان معدل التدفق الكتلي لـ (R-22) يزداد بزيادة درجة حرارة الدخول لطول وقطر ثابتين للانبوب الشعري. استخدم بعدئذ الرمز الحاسوبي للتنبوء بالجريان وانتقال الحرارة على امتداد انواع عدة من الانابيب الشعرية بمعنى اخر عدة اطوال و اقطار وموائع تثليج للانبوبين المبرد وغير المبرد. وجد في نتائج الانبوب الغير المبرد ان طول الانبوب لـ R-407C (R-32/125/134a(23/25/52)) اقصر من ذلك المطلوب لـ (R-22). لقد وجد (R-22) يتاخر تبخره مقارنة مع (R-407C). الحالة نفسها وجدت بالنسبة لـ (R-12) وبديله R-134a (CF3CH2F). توضح النتائج

النظرية ايضا بان طول الانبوب الشعري لة تاثير كبير على اداء المنظومة. عند زيادة الطول فان الهبوط في الضغط ودرجة الحرارة والكثافة تقل . بينما السرعة ونسبة الجفاف تزدادان.

## List of Symbols

$S_f$	General source term	
$x$	Dryness fraction	
$C, C_D$	Constants in turbulence model	
$I$	Turbulence intensity factor	
$k$	Turbulent kinetic energy	$(m/sec)^3$
$G$	Generation rate of turbulence energy	$kg/m.s^3$
$h$	Enthalpy	$kJ/kg$
$C_p$	Specific heat	$kJ/kg.K$
$r, z$	Polar coordinates	$m$
$u, v$	Components of velocity vector in $r$ and $z$ directions	$m/sec$
$P$	Pressure	$N/m^2$
$T$	Temperature	$^{\circ}C$
$K$	Thermal conductivity of refrigerant	$W/m.K$
$f$	General independent variable	
$\Gamma$	General diffusion parameter	$kg/m.sec$
$e$	Dissipation rate of turbulent kinetic energy	$m^2/sec^3$
$m_{eff}$	Effective dynamic viscosity	$kg/m.sec$
$t$	Shear stress	$N/m^2$
$k$	Von-Karman constant	
$\rho$	Density	$kg/m^3$
$S$	Prandtl number	
$l$	Length scale factor	
$\nu$	Kinematic viscosity	$m^2/sec$
$\Delta$	Difference between values	
in	Inlet conditions	
out	Outlet conditions	
f	Liquid phase	
g	Vapor phase	
t	Turbulent	
+	Dimensionless variable	
$r_{pipe}$	Radius of capillary tube	$mm$

## Abbreviations

CF3CH2F	1,1,1,2-tetrafluoroethane	
CFD	Computational fluid dynamics	

### Introduction

The capillary tube is a type of expansion device used in small vapour-compression refrigerating and air conditioning systems, located between the condenser and the evaporator. The function of the capillary tube is to reduce the high pressure in the condenser to low pressure in the evaporator. It is also used as an automatic flow rate controller for the refrigerant when varying load conditions and varying condenser and evaporator temperatures are encountered. Its simplicity, low initial cost, and low starting torque of compressors are the main reasons for its use. The capillary tube is commonly used as a constant area expansion device. It is a simple copper tube with an inner diameter of a few millimeters, but the flow inside these tubes is very complex, and the pressure drop has a strong influence on the performance of the whole system. Capillary tubes have been extended to larger units such as unitary air conditioners in sizes up to (10) tons of refrigerant [1].

Lin et al. (1990)[2] presented a steady-state, two-phase flow in capillary tubes. Five differential equations based on the drift flux model of two-phase flows were solved by using the runge-kutta method simultaneously. A comparison with experimental data for two-phase flow of R-12 flowing through capillary tubes, shows that the model is practical and can be used for selection of capillary tubes used in refrigerant system.

Chen. (1997)[3] presented a theoretical and experimental study

about capillary tube, an experimental test measure the pressure and temperature along the capillary tube to determine the under pressure of vaporization. The flow in the capillary tube was numerically modeled by dividing the flow into two regions, single phase and two-phase flow region used one dimensional with metastable phenomenon is account. The result indicated that the vaporization occurred near the capillary tube exit with strong heat transfer between the capillary tube and suction line.

Liang and Wong (2001)[4] attempted to exploit the possibility of applying the equilibrium two-phase drift flux model to simulate the flow of refrigerant in an adiabatic capillary tube. Their attempts are to compare predictions with experimental data of Li et al., 1990[5] and Mikol, 1963[1] for R12 and R134a. They presented the details of flow characteristics of R134a within a capillary tube, such as, distribution of pressure, void fraction, and dryness fraction and phases velocities. Their results showed a good agreement with the experimental data of Li et al., 1990 and Mikol, 1963. Gu et al. (2003)[5] analyzed and modeled the adiabatic flow in the capillary tube for R407C which is a non zeotropic mixed refrigerant and one of the alternatives to R22. They presented the equations of energy, continuity, and pressure drop through a capillary tube, and developed a mathematical model of the sub cooled flow region and the two-phase flow region by considering the homogenous model

and ignoring the metastable effect. They conclude that at the same working and geometric conditions, the mass flow rate of R407C is greater than R22 by (4%).

Muhsen (2007)[6] carried out an experimental and theoretical study about a capillary tube. He concluded from the experimental results that R600a requires a capillary tube shorter than that for R12 for the same inner diameter and as the ambient temperature increased, the compressor power increased and the capacity decreased. Also, the R600a can be operated with condensing pressures less than that of R12 for different ambient temperatures which makes less power consumption for R600a as compared with R12. This makes the coefficient of performance of the system working with R600a is higher than that of R12.

Many researchers have been investigated the capillary tube performance experimentally and theoretically. Most of these studies treated the flow as one dimensional viscous flow. They used several methods to solve a simplified form of the conservation equation of mass, momentum, and energy. None of the theoretical studies have solved the problem of the capillary tube using two dimensional Navier-stokes equations, and none of the previous experimental work has cooled the total length of the capillary tube. Therefore in the present work, a two dimensional study has been carried out to simulate the theoretical two-phase flow of the capillary tube using the conservation equation of mass, momentum, and energy equation as presented by Navier-stoke forms. The objective is to

study the performance of the capillary tube in an attempt to improve its duty in domestic refrigerator and air conditioning unit. This will be done through building a computer program to simulate the governing equation of flow and heat transfer in two dimensional geometry to predict the effect of capillary tube dimensions on the performance of domestic refrigerator and air conditioning unit. Obtaining a detailed values for temperature , pressure, density, dryness fraction, and velocity distribution in two dimensional geometry, and carrying out an experimental work to use its results to verify the theoretical simulation in order to make the computer code in a common use form and to select a capillary tube for a given application.

#### **Mathematical modeling**

The coordinate system used in this work is the cylindrical coordinate system. The usual radius ( $r$ ) and longitudinal coordinate ( $z$ ) are defined in figure (1), where ( $r$ ) and ( $z$ ) are the inner radius and the length of the capillary tube, respectively.

In order to solve the governing equations, several assumptions should be used. These are as follows :

- 1- Straight, horizontal (gravity effects are neglected), and constant inner diameter of the capillary tube is assumed.
- 2- Two dimensional geometry is considered.
- 3- The flow is assumed to be steady , incompressible, and turbulent .
- 4- Thermodynamics equilibrium (i.e. Metastable effect is neglected) [7].
- 5- Heat transfer to the surrounding is negligible.

6- Homogeneous flow (liquid and vapor velocities are assumed to be equal) [7].

The equations of conservation of mass, momentum, energy, turbulent kinetic energy (k), and turbulent energy dissipation rate ( $\epsilon$ ), can be written in a general form, as follows [8]:

$$\frac{1}{r} \left\{ \frac{\partial}{\partial z} (r u f) + \frac{\partial}{\partial r} (r v f) - \frac{\partial}{\partial z} \left( r \Gamma_f \frac{\partial f}{\partial z} \right) - \frac{\partial}{\partial r} \left( r \Gamma_f \frac{\partial f}{\partial r} \right) \right\} = S_f \quad \dots(1)$$

putting ( $f$ ) equals to unity, and ( $\Gamma_f$ ) and ( $S_f$ ) are equal zero, the above equation will represent the continuity equation.

$$\frac{1}{r} \left\{ \frac{\partial}{\partial z} (r r u) + \frac{\partial}{\partial r} (r r v) \right\} = 0 \quad \dots(2)$$

When ( $f$ ) represents the two velocity components (u and v), equation (1) represents the momentum equation in two dimensions.

$$\frac{1}{r} \left\{ \frac{\partial}{\partial z} (r u u) + \frac{\partial}{\partial r} (r v v) \right\} = \frac{1}{r} \left\{ \frac{\partial}{\partial z} \left( m_{eff} \frac{\partial u}{\partial z} \right) + \frac{\partial}{\partial r} \left( m_{eff} \frac{\partial u}{\partial r} \right) \right\} + S_u \quad \dots (3)$$

$$\frac{1}{r} \left\{ \frac{\partial}{\partial z} (r u v) + \frac{\partial}{\partial r} (r v v) \right\} = \frac{1}{r} \left\{ \frac{\partial}{\partial z} \left( m_{eff} \frac{\partial v}{\partial z} \right) + \frac{\partial}{\partial r} \left( m_{eff} \frac{\partial v}{\partial r} \right) \right\} + S_v \quad \dots (4)$$

Where the source terms ( $S_u$ ) and ( $S_v$ ) are given by,

$$S_u = \frac{\partial}{\partial z} \left( m_{eff} \frac{\partial u}{\partial z} \right) + \frac{1}{r} \frac{\partial}{\partial r} \left( r m_{eff} \frac{\partial v}{\partial z} \right) - \frac{\partial p}{\partial z} \quad \dots (5)$$

$$S_v = \frac{\partial}{\partial z} \left( m_{eff} \frac{\partial v}{\partial z} \right) + \frac{1}{r} \frac{\partial}{\partial r} \left( r m_{eff} \frac{\partial v}{\partial r} \right) - m_{eff} \frac{v}{r^2} - \frac{\partial p}{\partial r} \quad \dots (6)$$

Also,

$$m_{eff} = m + m_t, \quad m_t = \frac{C_m r k^2}{e} \quad \dots (7)$$

Putting ( $f$ ) equals to the enthalpy, equation (1) will represent the energy equation.

$$\frac{1}{r} \left\{ \frac{\partial}{\partial z} (r u h) + \frac{\partial}{\partial r} (r v h) \right\} = \frac{1}{r} \left\{ \frac{\partial}{\partial z} \left( r \Gamma_h \frac{\partial h}{\partial z} \right) + \frac{\partial}{\partial r} \left( r \Gamma_h \frac{\partial h}{\partial r} \right) \right\} + S_h \quad \dots (8)$$

Also,

$$\Gamma_h = \frac{k}{C_p} + \frac{m_t}{S_h} \quad \dots (9)$$

Where,

$$h = h_s + x h_{fg} \quad \dots (10)$$

$$h_s = C_p \Delta T \quad \dots(11)$$

Due to the non-linear behavior of the dryness fraction (x) along the length of the capillary tube, a parabolic profile is assumed following [9]:

$$x = x_o (z_r)^2 \quad \dots (12)$$

Where,

( $x_o$ ) is the dryness fraction at the end of the capillary tube and it is given by,

$$x_o = \frac{h_{in} - h_{f,out}}{h_{fg,out}} \quad \dots (13)$$

( $Z_r$ ) is the ratio of the location of a specific node to the length of capillary tube.

The density for the flow is given by [10],

$$r = \frac{1}{\frac{x}{r_g} + \frac{1-x}{r_f}} \quad \dots (14)$$

Here ( $\rho_f$ ) represent the liquid density and ( $\rho_g$ ) is the vapor density. The source term ( $S_h$ ) is set to zero.

$$S_h = 0 \quad \dots (15)$$

The general modified form of ( $k\epsilon$ ) model can be written as follows[8]:

For the capillary tube, the following boundary conditions are assumed and problem is solved for the upper half of the tube due to symmetry:

**Upstream Boundary Conditions:**

The distribution of all flow variables needs to be specified at upstream boundaries [11].

$$u_{up} = u_{in} \quad v_{up} = 0$$

$$k_{up} = I \times (u_{in})^2 \quad e_{up} = \frac{(k_{up})^{1.5}}{I \times r_{pipe}}$$

**Downstream Boundary Conditions**

Normally, the velocities are only known where the fluid enters the calculation domain. At downstream, the velocity distribution is decided by the flow field within the domain. For incompressible flow, the gradients normal to the downstream surface of all quantities are assumed to be zero [11].

$$\frac{\partial f}{\partial z} = 0$$

**Wall Boundary Conditions**

The wall is the most common boundary encountered in confined fluid flow problems. The no-slip condition ( $u = v = 0$ ) is the appropriate condition for the velocity components at solid walls. In the case of turbulent flow, the calculation of shear stress near the wall needs a special treatment. This is due to the existence of boundary layers, across which a steep variation of flow properties occurs and the standard ( $k\epsilon$ ) model becomes inadequate. In order to adequately avoid these problems, it would be necessary to employ a fine grid near the wall, which would be expensive. An alternative and widely employed approach is to use a formula which known as “wall function”[11].

The implementation of wall boundary conditions in turbulent flows required the evolution of the following parameters as given below:

$$y^+ = \frac{y_p}{n} \sqrt{\frac{t_w}{r}} \quad \dots (16)$$

$$u^+ = \frac{1}{k} \ln(Ey^+) \quad \dots (17)$$

$$t_w = r C_m^{1/4} k_p^{1/2} u_p / u^+ \quad \dots (18)$$

$$k_p = \left( t_w u_p - r C_m^{3/4} k_p^{3/2} u^+ \right) / y_p \quad \dots (19)$$

$$e_p = C_m^{3/4} k_p^{3/2} / (k \Delta y_p) \quad \dots (20)$$

$$q_w = -r C_p C_m^{1/4} k_p^{1/2} (T_p - T_w) / T^+ \quad \dots (21)$$

$$T^+ = s_t \left( u^+ + P \left[ \frac{s_l}{s_t} \right] \right) \quad \dots(22)$$

Where, ( $y_p$ ) is the distance of the near wall node (P) to the solid surface and near-wall flow is taken to be laminar if ( $y^+ \leq 11.63$ ). The wall shear stress is assumed to be entirely viscous in origin. If ( $y^+ > 11.63$ ), the flow is turbulent and the wall function approach can be used.

( $\kappa$ ) is Von Karman's constant (0.4187) and (E) is an integration constant that depends on the roughness of the wall. For smooth wall (E) has a value of (9.793). Other empirical constants appear in ( $k-\epsilon$ ) model and wall function are given in Table (1).

A computational technique for the solution of the continuity, momentum, energy, and turbulence quantities, is performed to obtain the discretization form for these equations. These discretization equations are solved by SIMPLE algorithm with power-law scheme. A computer program based on this algorithm and uses Fortran 90 language, was built to meet the requirements of the problem. A staggered grid in which the velocities staggered midway between the grid intersections, was used to obtain the numerical results. The grid number was (50,10) in (z, r) direction, respectively, see Figure (2).

### Experimental Apparatus and Rig Layout

The experimental rig was constructed to measure the pressure and temperature along the capillary

tube and to use the data from the measurements for comparison with the theoretical part. The rig was constructed to facilitate the measurement with a cooled or non cooled capillary tube, which can be seen in Figure (3).

Two tests were carried out in the present study. The first test was applied to a capillary tube with out cooling i.e. adiabatic capillary tube as found in the normal operating conditions. The second test is applied to a capillary tube with cooling. The cooling was done by placing the capillary tube in contact with return line from the evaporator, and both lines were insulating.

### Results and Discussion

The experimental work was directed into two ways, the first is studying the effect of increasing the inlet temperature on the outlet pressure and temperature and the refrigerant effect via the mass flow rate. The second is to study the cooling effect of the capillary tube walls using the suction vapor refrigerant line.

Figure (4) shows a comparisons between the CFD results with the experimental data for pressure and temperature profile along the capillary tube. Both results represent the variation of temperature and pressure for a range of inlet temperatures (29 – 41 °C). The effect of the inlet temperature is clear in these plots that show the pressure difference along the capillary is increased as the inlet temperature and pressure increased. This may lead to increase the mass flow rate of the refrigerant that pass through the compressor. The temperature drop is derived by the pressure difference

along the capillary tube developed due to the throttling action as the liquid– gas moves from condenser to the evaporator.

The present numerical results are compared with the numerical predictions of Jung et al. [13] and Ooi et al. [15] and the experimental data for Sami et al. [14] for the temperature, pressure dryness fraction and velocity profile along the capillary tube. These comparisons are shown in Figure (5), (6), (7) and (8) which reveals small differences between both results for different refrigerants.

The present computer code was employed to predict several cases using several refrigerants with different lengths and diameters for both cooled and non cooled capillary tubes. The non cooled tube results are first presented.

Figure (9) shows the velocity vectors distribution along the capillary tube. The results appear that the value of the velocity increased along the tube where more liquid flashes due to pressure drop. The development of the flow along the capillary tube length is clearly shown in sections III and IV.

Figure (10) and (11) show the pressure and temperature distribution along the capillary tube for different lengths. The results show the pressure drop increases with increasing the length of capillary tube. The reason for the pressure drop is mainly due to strong flow turbulence inside the capillary tube length and also due to the drop of temperature along the tube. The gradient drop in temperature is due to the phase change of the liquid to vapor and the absorption of the latent

heat of vaporization. As the capillary tube length increases, the drop in the pressure and temperature increases, but this length is limited by the dryness at exit. The dryness should be minimum to reduce the liberation of the latent heat of flashing of refrigerant liquid and store it to the evaporator to exchange heat with the cooling agent, air in the present study.

Figure (12) shows the velocity distribution along the capillary tube for different lengths. The velocity increases with capillary tube length. The density of refrigerant decreases as the vapor fraction increases and this lead to increase the velocity up to the chock flow. This phenomena is undesirable and it should be prevented by selection the tube length to be shorter.

Figure (13) shows the density and velocity distribution along the capillary tube for different refrigerants. The result show that the density decreases as the length increases, and this lead to increase the velocity to satisfy the law of continuity.

Figure (14) shows the relation between pressure and velocity. The result appears that the pressure drop increases with velocity of refrigerant and this leads to increase the drop in density, resulting in an increase in the velocity while the flow advances forward. The velocity for (R-22) is close to (R-407C) because their critical densities are close to each other. The velocity of (R-12) is also found to be close to (R-134a) for similar reasons.

The effect of the cooling on the performance of the capillary tube is presented in Figures (15) and (16). The cooling occurred on a part of the

capillary tube length as in Figure (15) and then for the total length as in Figure (16). The result appears that the cooling has a little effect on the performance of the capillary tube. This may be due to the high flow velocity in the tube which limited the heat exchange between the refrigerant and its close boundaries.

### Conclusions

The following conclusions can be adopted as a result of studying two-phase flow of the refrigerant in the capillary tube numerically and experimentally.

1. The length of capillary tube has a large effect on performance of capillary tube, while the diameter of capillary tube has a less effect.
2. From the dryness fraction distribution curves along the same capillary tube, it is found that the alternative refrigerant vaporizes faster than the traditional refrigerant.
3. Pressure drop for alternative refrigerant is higher than that for traditional refrigerant, and the length required for alternative refrigerant is less than the traditional refrigerant.
4. The velocity increased along the capillary tube downstream from the inlet, also with increasing the drop of both density and pressure of the refrigerant.
5. Increasing the inlet temperature of capillary tube leads to increase the mass

flow rate of the refrigerant and compressor work.

6. The results show that cooling part or all the length of the capillary tube has a little effect on its performance.
7. Good agreement between the present work and the numerical and experimental data that presented by other researchers was found, and this enables the theoretical model to predict the performance of a capillary tube of different lengths and with different refrigerants.

### References

- [1] Corberan, J. M., Fuentes, D., and Gonzalez, J., "*Numerical calculation of mass flow rate in capillary tubes using ART*", Advanced Simulation Software, Int .Ref . Con. Proceeding, Purdue University,(2006).
- [2] Li, R. Y., Lin, S., and Chen, Z.H., "*Numerical modeling of thermodynamic non-equilibrium flow of refrigerant through capillary tubes*", ASHRAE Transactions 96, (1990), pp. 542-549.
- [3] Chen, D., "*Flashing flow of refrigerant HFC-134a through adiabatic capillary tube*", Ph. D. Thesis, Concordia University, Mechanical Engineering Department, (1997).
- [4] Liang, S. M., and Wong, T. N., "*Numerical modeling of two phase Refrigerant flow through adiabatic capillary tubes*", Applied Thermal Engineering, 21, (2001), PP.1035-1048. [5] Gu, B., Li, Y., Wang, Z., and Jing, B., "*Analysis on the Adiabatic Flow of R407c in*

- Capillary Tube*", Applied Thermal Engineering, 23, (2003), pp.1871-1880.
- [6] Muhsen, M. M., "*Experimental and theoretical study of flowing refrigerants R12 and R600a in an adiabatic capillary tube considering metastable region*", M.Sc. Thesis, University of Technology, Mech. Eng. Department, (2007).
- [7] Xu, B., and Bansal, P. K., "*Non-adiabatic capillary tube flow: a homogeneous model and process description*", Applied Thermal Engineering, 22, (2002), pp.1801-1819.
- [8] Gosman, A.D, and Ideriah, F, J, K., "*A general computer program for two-dimensional, turbulent, recirculating flows*", Department of Mechanical Engineering Imperial College London (1983).
- [9] Sinpi boon, J., and Wongwises, S., "*Numerical investigation of refrigerant flow through non-adiabatic capillary tubes*", Applied Thermal Engineering 22, (2002), pp. 2015-2032.
- [10] Agrawal, N., and Bhattacharyya, S., "*Adiabatic capillary tube flow in a transcritical carbon dioxide heat pump*", Gustav Lorentzen Conference on Natural Working Fluids, Trondheim, Norway, (2006).
- [11] Versteeg, H.K., and Malalasekera, W., "*An introduction to computational fluid dynamics-the finite volume method*", Longman group Ltd., (1995).
- [12] Awbi, H. H., "*Ventilation of building*", Department of Construction Management and Engineering, University of Reading, London (1991).
- [13] Jung, D., Park, C., and Park, B., "*Capillary tube selection for HCFC22 alternatives*", International Journal of Refrigeration, 22, (1999), pp. 604-614.
- [14] Sami, S. M., Maltais, P. E., and Desjardins, D. E., "*Influence of geometrical parameter on capillary behavior with new alternative refrigerants*", Int. J of Energy Research, (2005).
- [15] Ooi, K. T. and Wong, T. N., "*Adiabatic capillary tube expansion device a comparison of the homogeneous flow and the separated flow model*", Applied Thermal Engineering, 16, (1996), pp. 625-634.

**Table (1) Empirical constants in the boundary conditions [12]**

C	$C_D$	I	
0.09	1.0	0.03	0.005

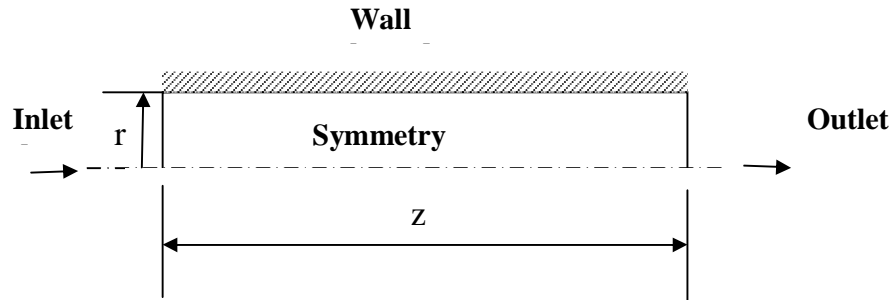


Figure (1) the capillary tube with its boundary conditions.

**Inlet boundary:**

$$u_{up} = u_{in}$$

$$v_{up} = 0$$

$$k_{up} = I \times (u_{in})^2$$

$$(1.5)$$

**Outlet boundary:**

$$\frac{\partial f}{\partial z} = 0$$

**Symmetry boundary:**

$$\frac{\partial f}{\partial r} = 0$$

**Wall boundary:**

$$\frac{\partial h}{\partial n} = 0$$

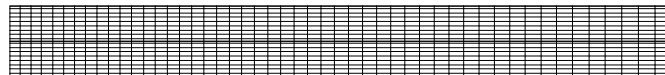
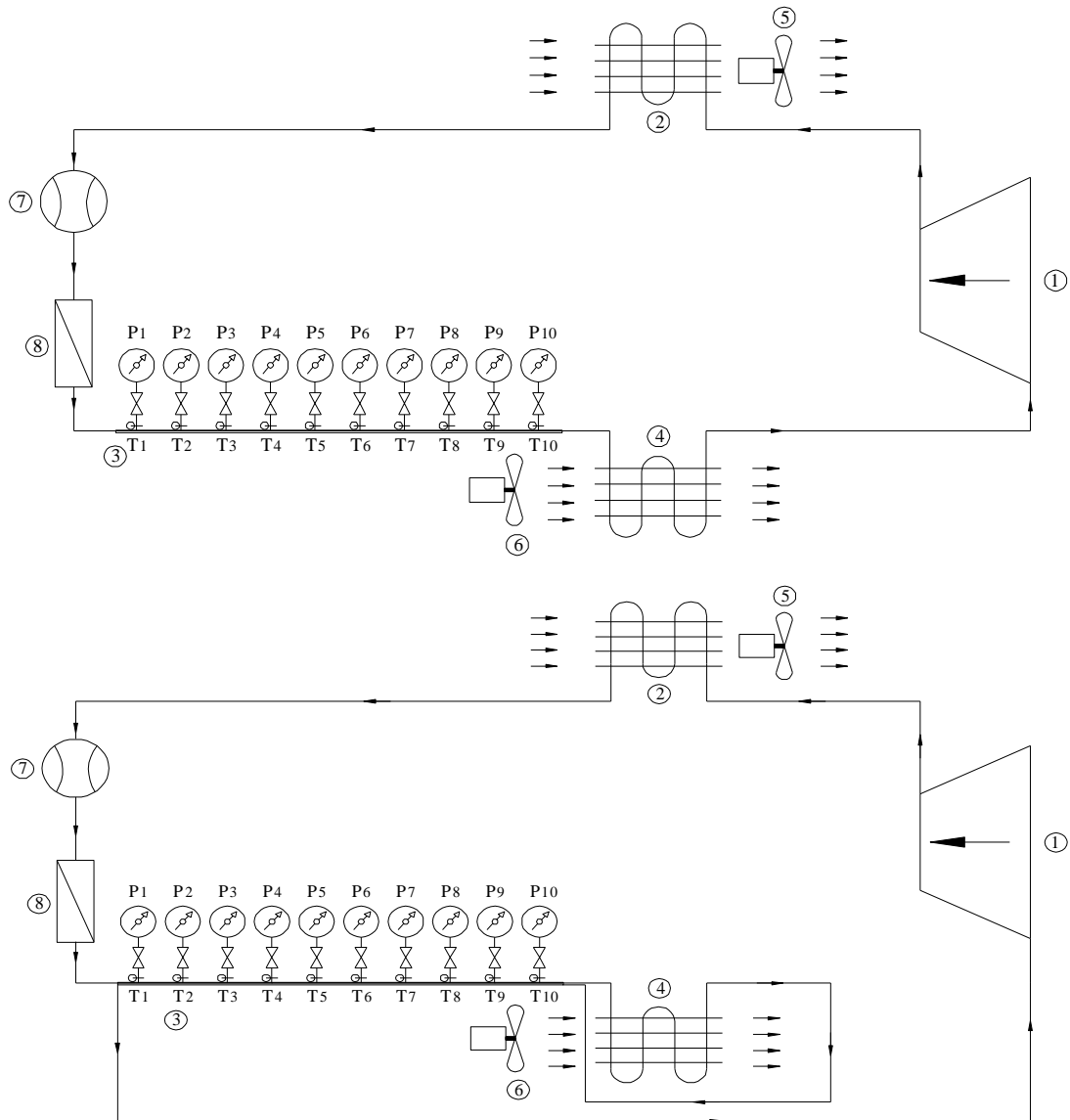


Figure (2) the grid used for capillary tube (Nz, Nr).



1	Compressor
2	Condencer
3	Capillary Tube
4	Evaprator
5	Condenser Fan
6	Evaprator Fan
7	Rotam eter
8	Filter
9	P1.....P10 Pressure Gauge
10	T1.....T10 Therometer

Figure (3) Schematic diagram of the split unit with adiabatic and non-adiabatic capillary tube.

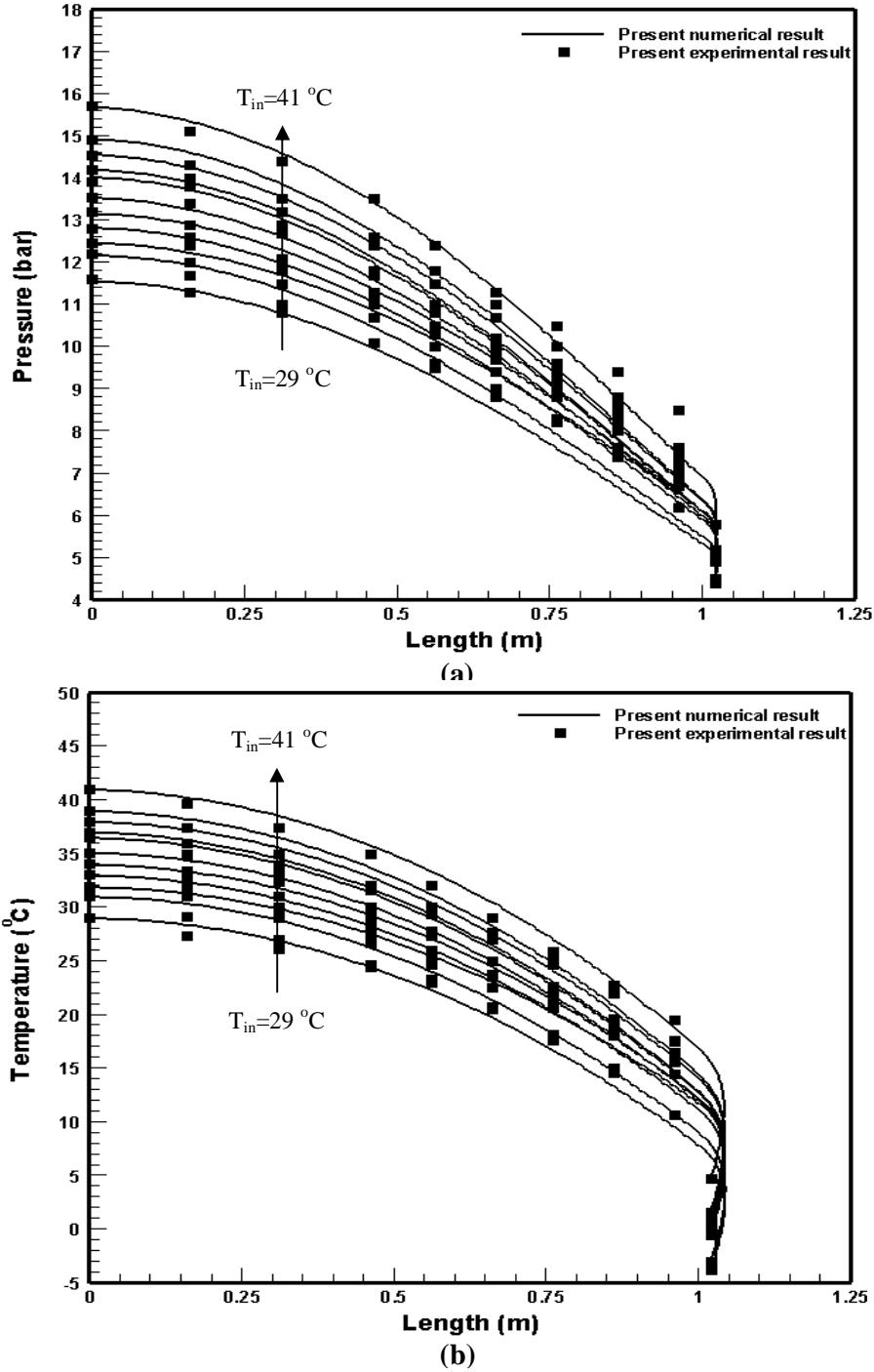


Figure (4) Comparisons of the present numerical results with the experimental data for pressure (a) and temperature (b) distribution along the capillary tube for different inlet temperatures at constant pressure in the evaporator.

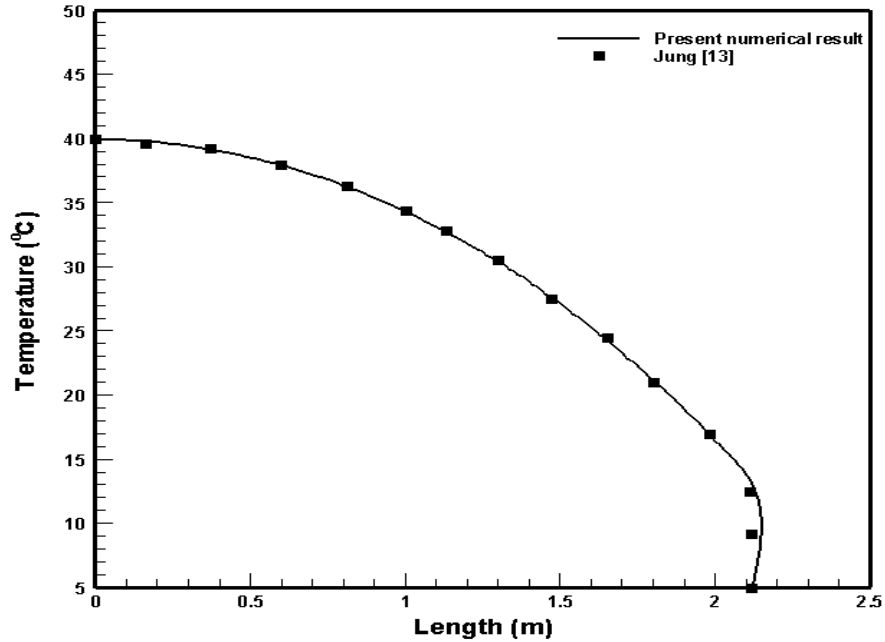


Figure (5) Comparison of temperature distribution along the capillary tube between the present work and numerical work for Jung [13] for R-22.

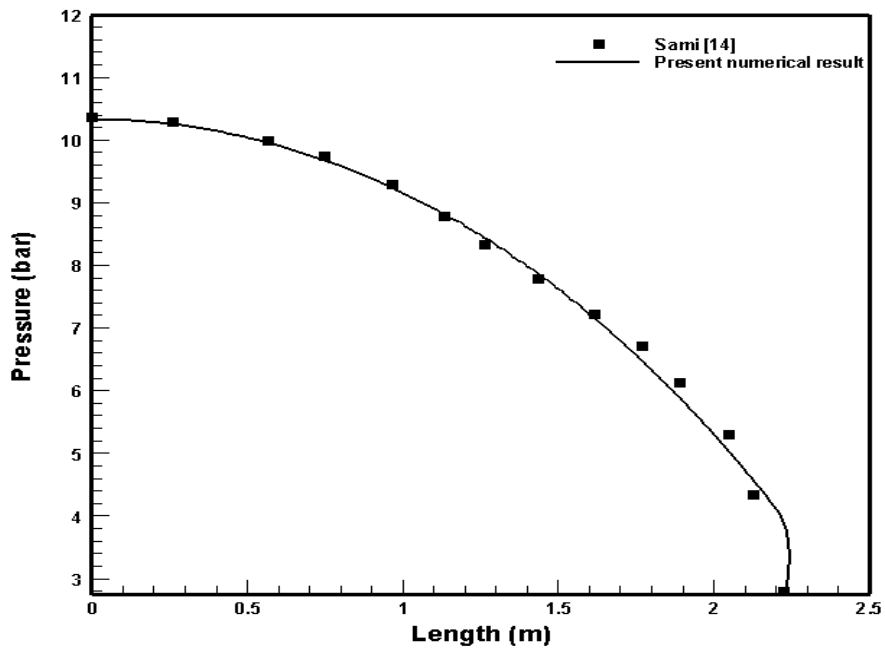


Figure (6) Comparison of pressure distribution along the capillary tube between the present work and experimental work for Sami [14] for R-407C.

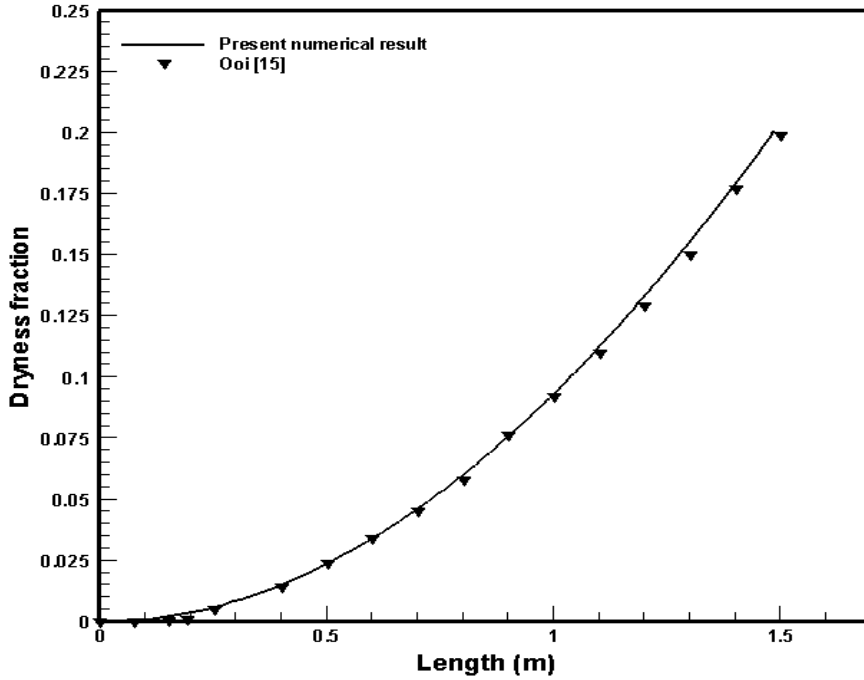


Figure (7) Comparison of dryness distribution along the capillary tube between the present work and numerical work for Ooi [15]

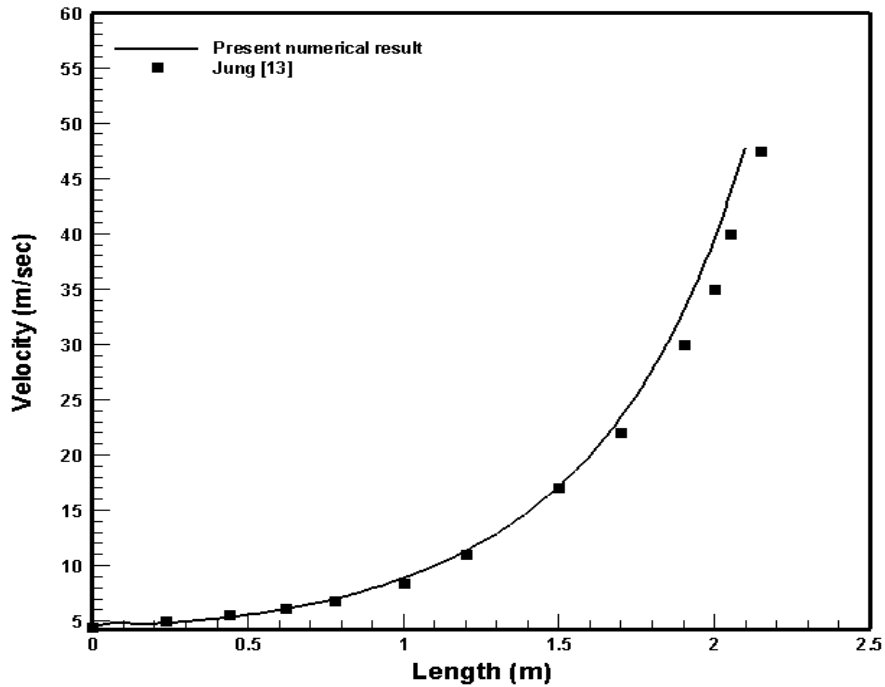


Figure (8) Comparison of velocity distribution along the capillary tube between the present work and numerical work for Jung [13] for R-22.

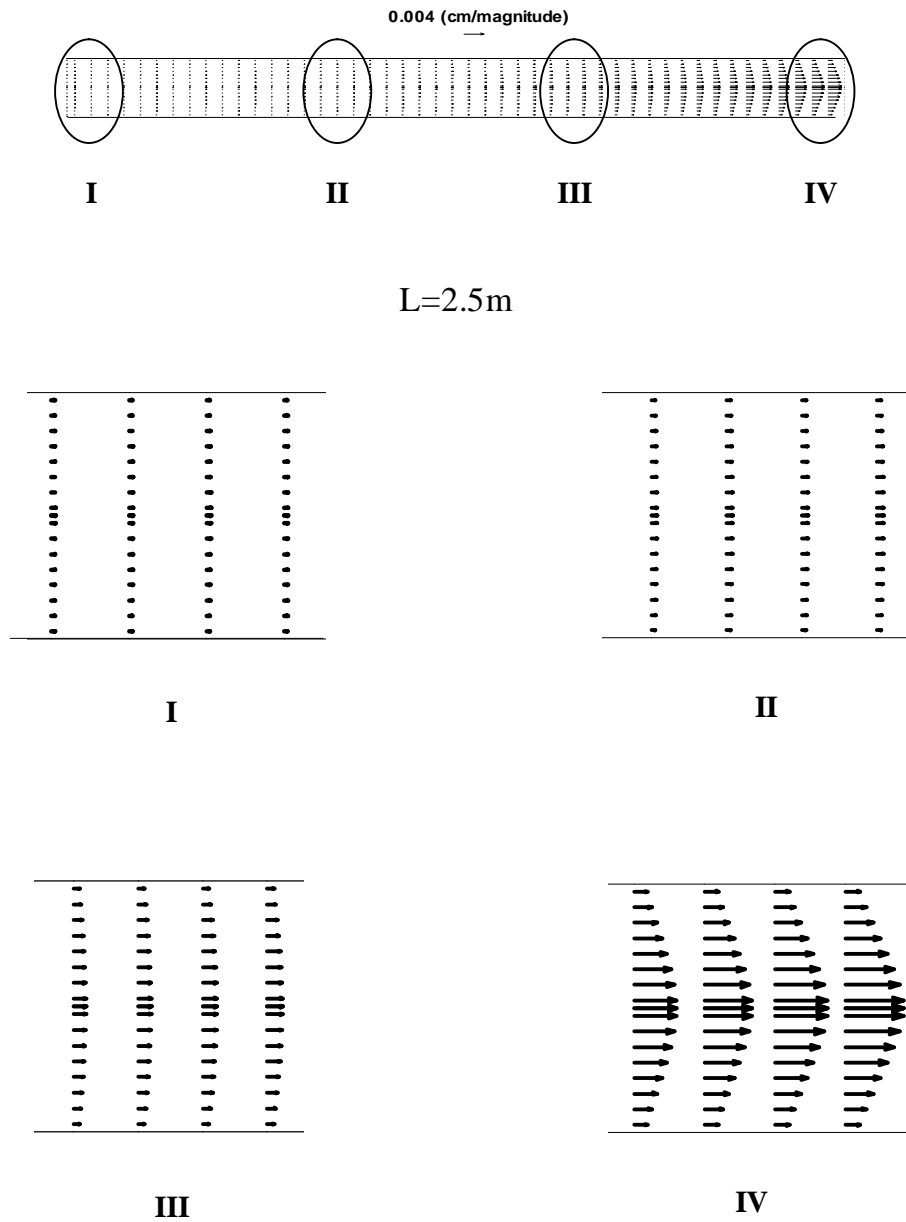


Figure (9) Velocity vector distribution along the capillary tube for R-22.

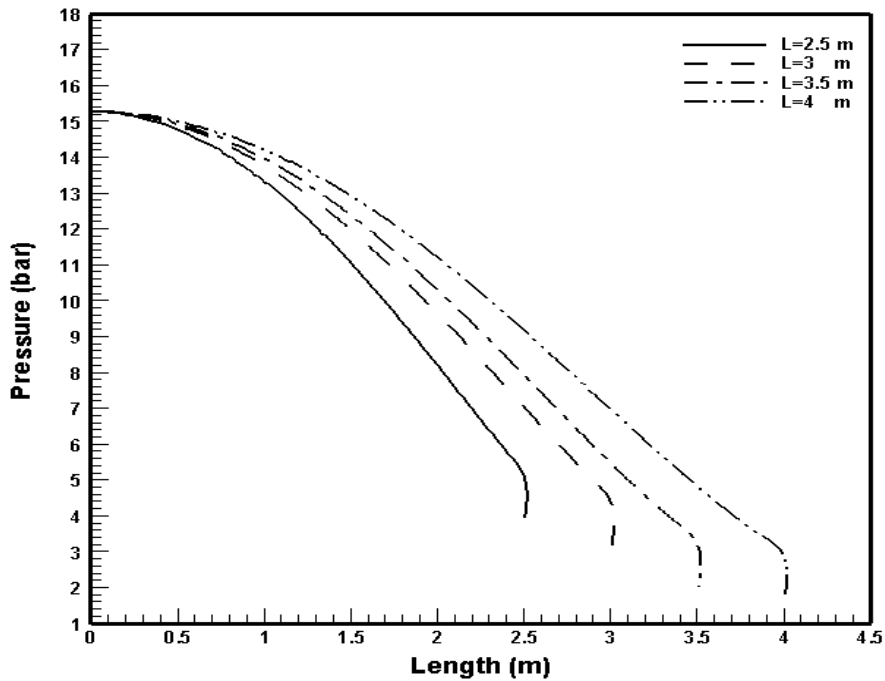


Figure (10) Pressure distributions along the capillary tube for different lengths for R-22.

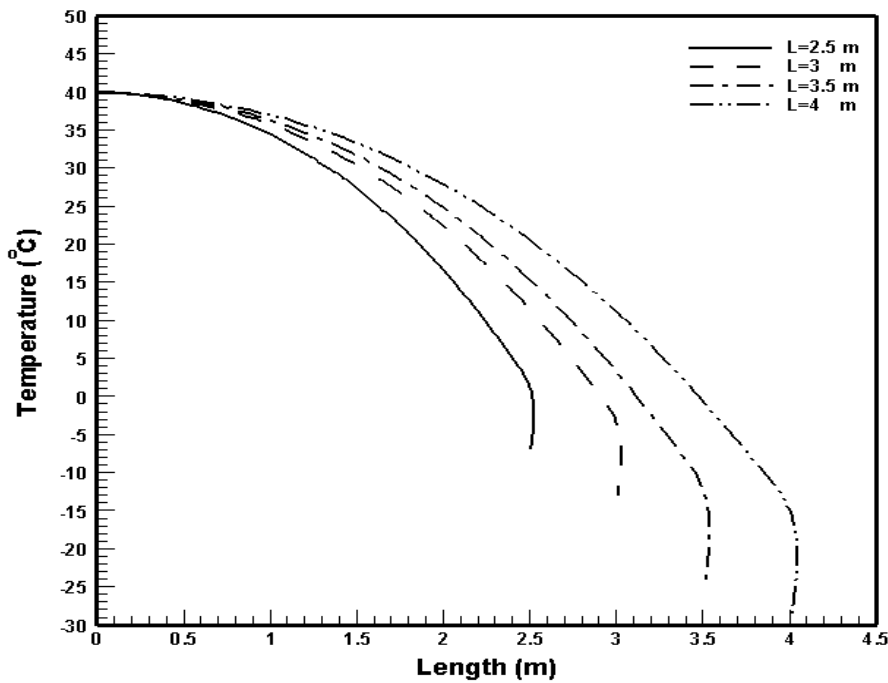


Figure (11) Temperature distributions along the capillary tube for different lengths for R-22.

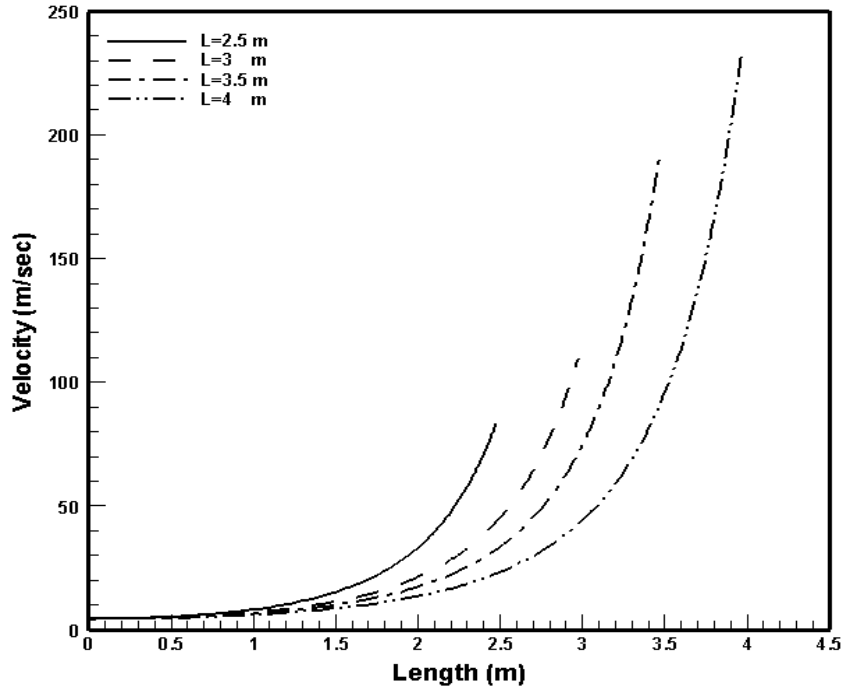


Figure (12) Velocity profile along the capillary tube for different lengths for R-22.

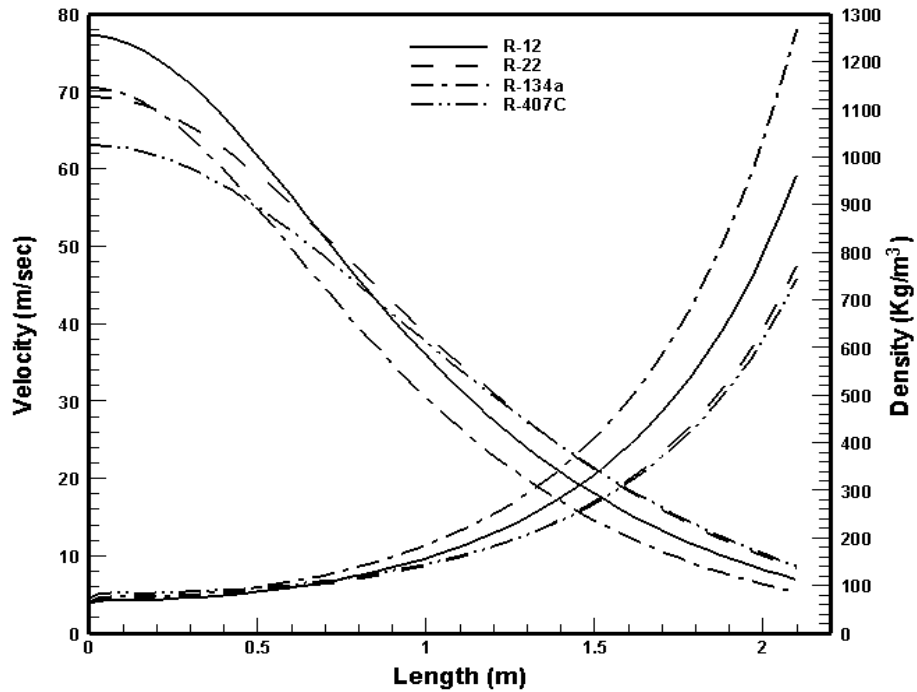


Figure (13) Density and Velocity distributions along the capillary tube for different refrigerants.

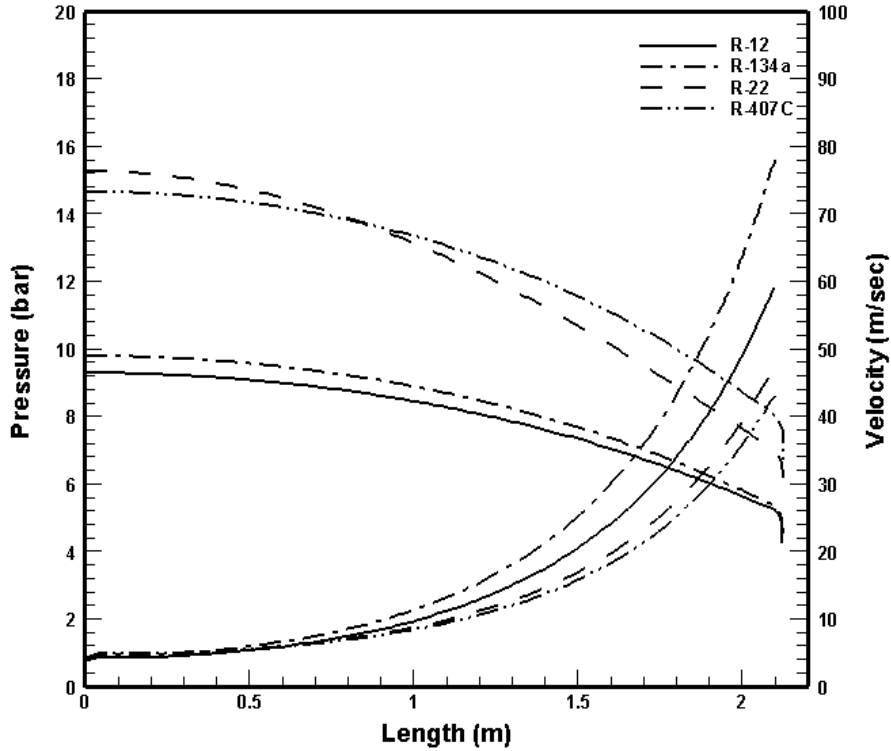


Figure (14) Pressure and Velocity distributions along the capillary tube for different refrigerants.

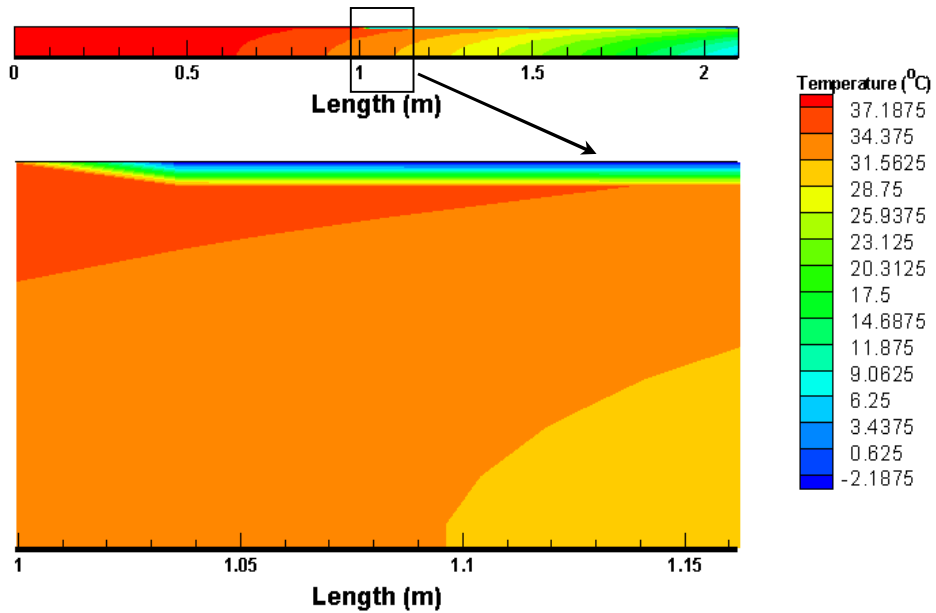


Figure (15) Effect of cooling part of capillary tube surface on its performance.

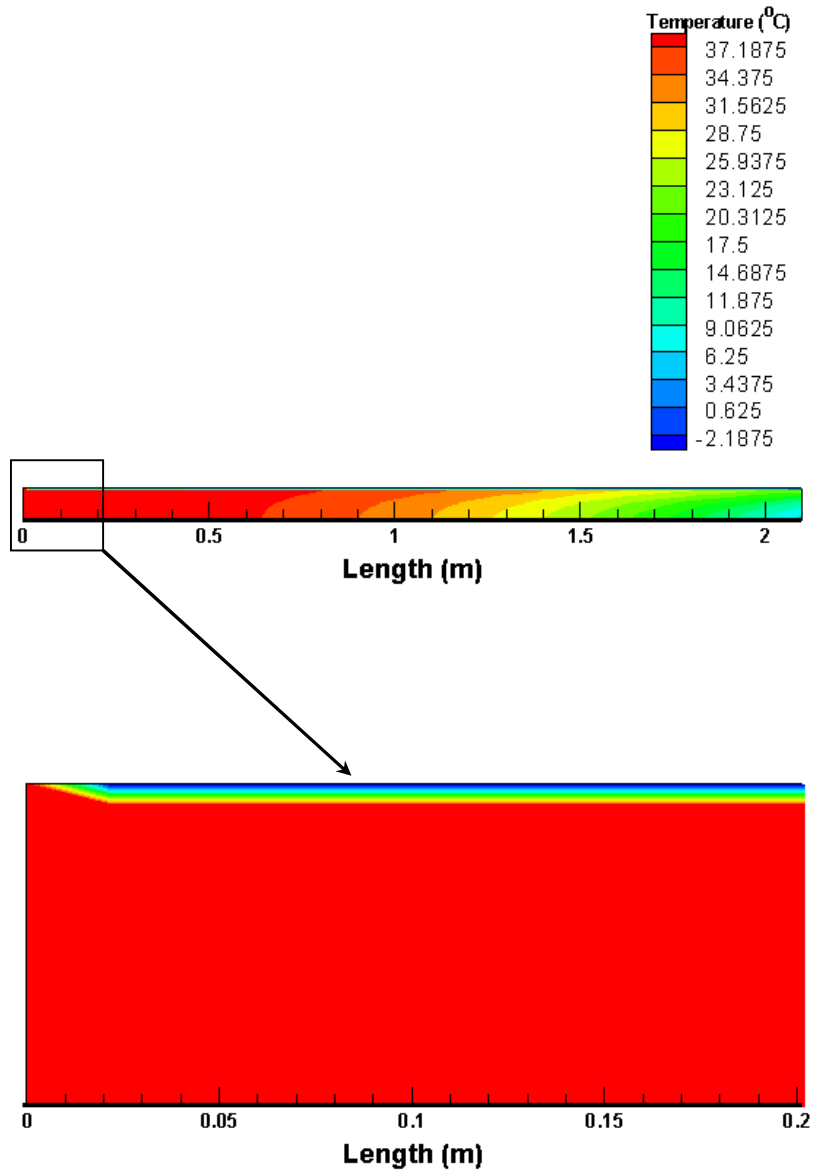


Figure (16) Effect of cooling capillary tube surface (all surface) on its performance.